Bright Object Protection Mechanisms for STIS

M. Clampin
May 14, 1997

ABSTRACT

The STIS bright object protection mechanisms onboard STIS are described, together with the characteristics and MAMA damage mechanisms.

1. Introduction

In common with most photon counting detectors it is possible to damage the MAMA detectors on STIS by subjecting them to excessive light levels. STIS is a versatile instrument which offers a wide range of spectral resolutions from 26 to 10^5 and a UV/Visible imaging capability. Given this range of capabilities, the STIS MAMA detectors will be will be used to observe a very diverse range of sources, many of which could potentially over-illuminate the detectors (see ISR 96-24). In addition to the possibility of over-illuminating a MAMA by observing an excessively bright source, since the STIS MAMA detector systems are not protected by shutters, there is also the possibility of inadvertently over-illuminating the detectors during internal operation of the instrument not directly related to the observation. Typical examples are the movement of the Mode Selection Mechanism (MSM) to select gratings (see STIS Instrument Handbook), or illumination by the bright earth during occultation. The MAMAs are currently baselined to be operated at their nominal operating voltages all the time, so even CCD science observations which involve an MSM move have the potential to inadvertently over-illuminate the MAMA detectors. The rules governing the use of bright object protection mechanisms for the STIS MAMA detectors need to be carefully specified to ensure that all contingencies are covered.

In order to protect the MAMA detectors, the STIS IDT have defined a Constraints and Restrictions Document (CARD) item to summarize the global and local damage levels for STIS MAMA detectors. These CARD restrictions are currently defined as:

a) The STIS Multi-Anode Micro-Channel Array (MAMA) must not be exposed to a

light source which would result in the following limits being exceeded:

- Global count rate limit of $1.5x10^6$ for greater than 1 second
- Local input count rate limit of 500 counts/low-res-pixel/sec (for FUV and NUV MAMAs) in an area encompassing 4 or more low-res (25x25 μm) pixels for greater than 30 seconds.

In this ISR we address the hardware and flight software related aspects of the STIS Bright Object Protection Scheme which has been implemented to ensure that the CARD is never violated. In Section 2 we discuss the design of the STIS MAMA detector and signal processing electronics, and review the shuttering options available to each detector. Section 3, covers the damage mechanisms which typically result from over-illuminating a MAMA detector. Section 4 and Section 5, summarize the mechanisms of the global and local count rate monitors, respectively.

2. STIS Instrument Design

STIS MAMA Detector Design

The STIS MAMA detectors are photon counting detectors which incorporate a microchannel plate (MCP) gain stage to multiply single photoelectrons to a detectable signal level of ~$4x10^5$ electrons. Microchannel plates are wafers of glass capillaries, where each capillary operates as a Channel Electron Multiplier. The principles and operation of MCPs has been described in detail by Eberhardt (1980) and Wiza (1979).

The primary benefits afforded by the STIS MAMAs, in comparison with existing HST spectroscopic detectors such as the GHRS and FOS, are high spatial resolution, large area, and 2-dimensional imaging formats. The MAMAs do not have the dynamic range capabilities of the one-dimensional FOS and GHRS digicon detectors, but exceed the dynamic range of the FOC. STIS has two different types of MAMA detector, one optimized for FUV imaging and one for NUV imaging. These designs are shown below in Figure 1 and Figure 2.

The FUV MAMA design comprises an opaque CsI photocathode deposited directly on the face of a curved MCP, followed by a fine-fine multi-anode array which encodes the spatial position of the incident photoelectron. Photoelectron collection efficiency is optimized by the use of a repeller wire located in front of the MCP. The repeller ensures that photoelectrons, produced by photons incident upon the front face of the MCP, are returned quickly to an adjacent MCP channel by the repeller's electric field. The FUV MAMA detector's entrance window is tilted with respect to the incident optical beam, in order to reduce lateral color in the FUV band images.

Figure 1: A schematic showing the design of the STIS FUV MAMA detector

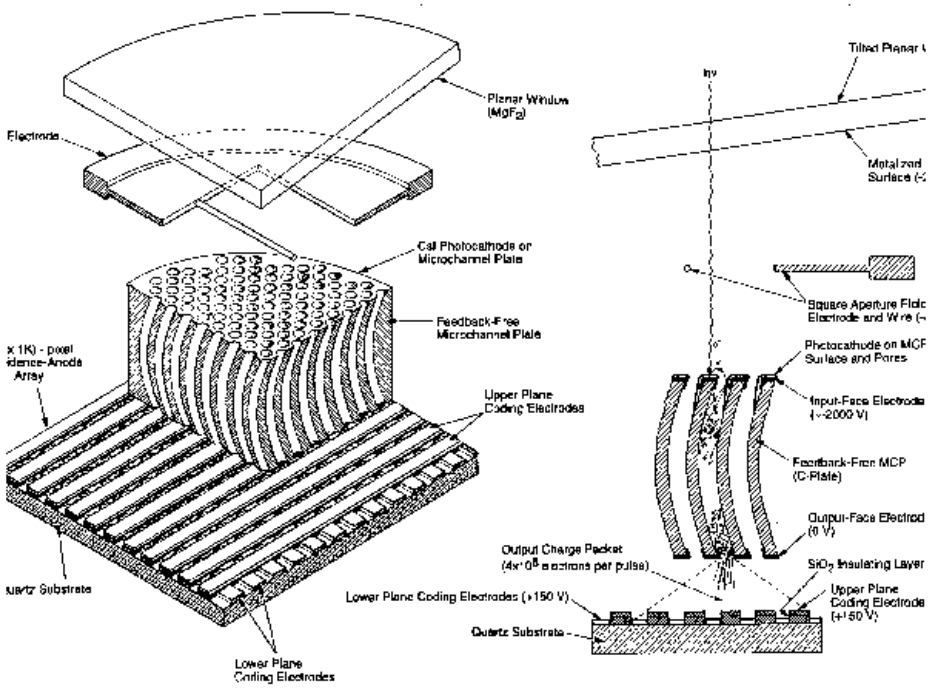

In contrast, the NUV MAMA has a semi-transparent Cs_2Te photocathode deposited on the back side of the detector's entrance window, but otherwise the same basic detector design. A potential across the window-MCP gap proximity focuses photoelectrons onto the MCP face. The spatial uncertainty resulting from lateral photoelectron drift between the photocathode and the MCP results in a slightly lower spatial resolution for the NUV MAMA, compared to the FUV MAMA.

Both the FUV and NUV MAMAs, in their baseline design, employ a curved MCP as the gain stage of the detector. Curved MCPs offer the benefits of high gain from a single MCP, combined with high local dynamic ranges, compared to chevron MCP stacks and improved ion feedback suppression. The MAMA MCPs have 12.5 μm channel diameters on 14 μm centers, so each anode pixel maps to approximately three MCP channels. The MAMA MCPs are operated in the gain saturated regime, where the pulse height distribution is gaussian, with a modal gain of ~$4x10^5$ electrons. Thus, the detectors equally weight all photons, the precondition for photon counting.

Figure 2: A schematic showing the design of the NUV MAMA

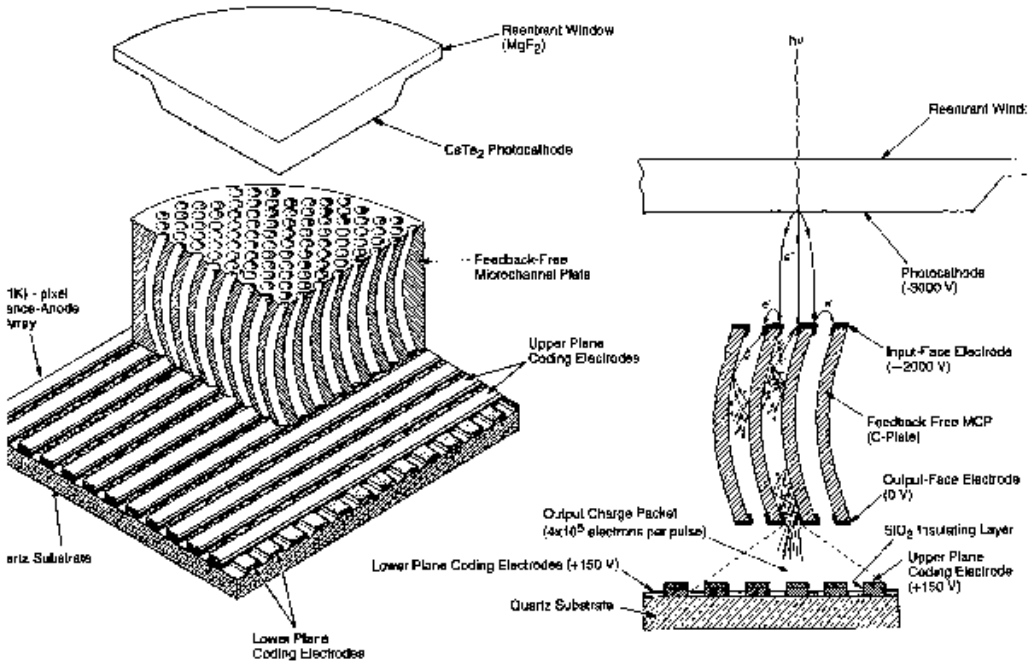

MAMA Detector Electronics

The MAMA signal processing electronics and their control hardware are shown schematically in Figure 3. The interface to the detector's anode wires is an array of charge amplifiers which integrate the ~$4x10^5$ electron charge packets and output them to a pulse height discriminator which thresholds out the smaller pulses. These smaller pulses typically correspond to the low gain tail of the MCPs pulse height distribution. Typical values for the discriminator setting are equivalent to an electron gain of $2x10^5$ electrons. Pulses passed by the discriminator are decoded by custom Application Specific Integrated Circuit (ASIC) decoder chips (Kasle 1992), which determine the X,Y coordinates of an event on the basis of the anode wires triggered and pulse selection criteria. The decode circuit latches for 260 nano-seconds every time an event is processed, during which time no other events can be processed. It is this deadtime which defines the performance of the signal processing electronics at high input count rates.

A number of counters are used to time the processing of events and also monitor processing rates. The OR counter counts all events passed by the discriminator circuit and is used to time event processing in the decode chip. The OR counter is also used by the Global Software Monitor to shutdown the detector in the event of over-illumination (see Section 4). Events which fall on the detector array, including the decode area, and which pass additional thresholding and fold distribution criteria are classed as EVENTS (EV). A subset of the EVENTS which lie in the active area of the detector are classed as VALID

EVENTS (VE). In general some events will fall on the decode area of the anode since most STIS observing modes do not have aperture masking to prevent this. These events are detected on one of the anode wires (W, X, Y and Z) but are rejected by the decode chip because there is no coincidence between the W, X, Y and Z anodes in the decode areas. The decode chips, known as ASICS, have a paralyzable deadtime of 260 ns. Thus, the relationship between true i.e. input OR counts and observed OR counts is

$$OR_{observed} = OR_{true} * \exp(-1 * OR_{true} * 260\ ns).$$

The relationship between VE and OR counts has been determined by Vic Argabright to be

$$VE_{observed} = VE_{observed}/OR_{observed} * OR_{true} * \exp(-1 * OR_{true} * 280\ ns),$$

where the ratio $VE_{observed}/OR_{observed}$ is 0.77 for full illumination. These relationships are shown in Figure 4.

In addition to the timing considerations for the signal processing electronics, there is a limitation of 300,000 counts/sec for the rate at which the MCE can process events from the signal processing electronics. If the photon event rate is higher than 300,000 counts/ sec, some events will not be processed, and lost. When operating in time-tag mode the restriction is 30,000 counts/sec.

Figure 3: Schematic illustration of the MAMA signal processing electronics

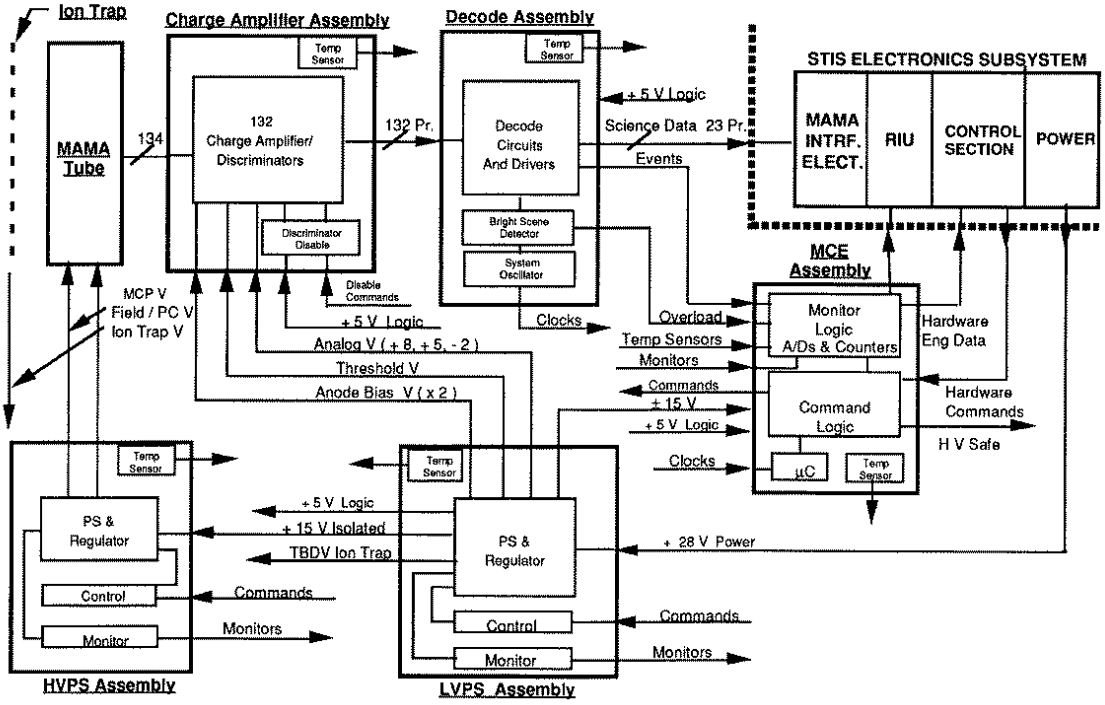

Figure 4: Plot showing the MAMA VE and OR observed rate vs. OR input rate.

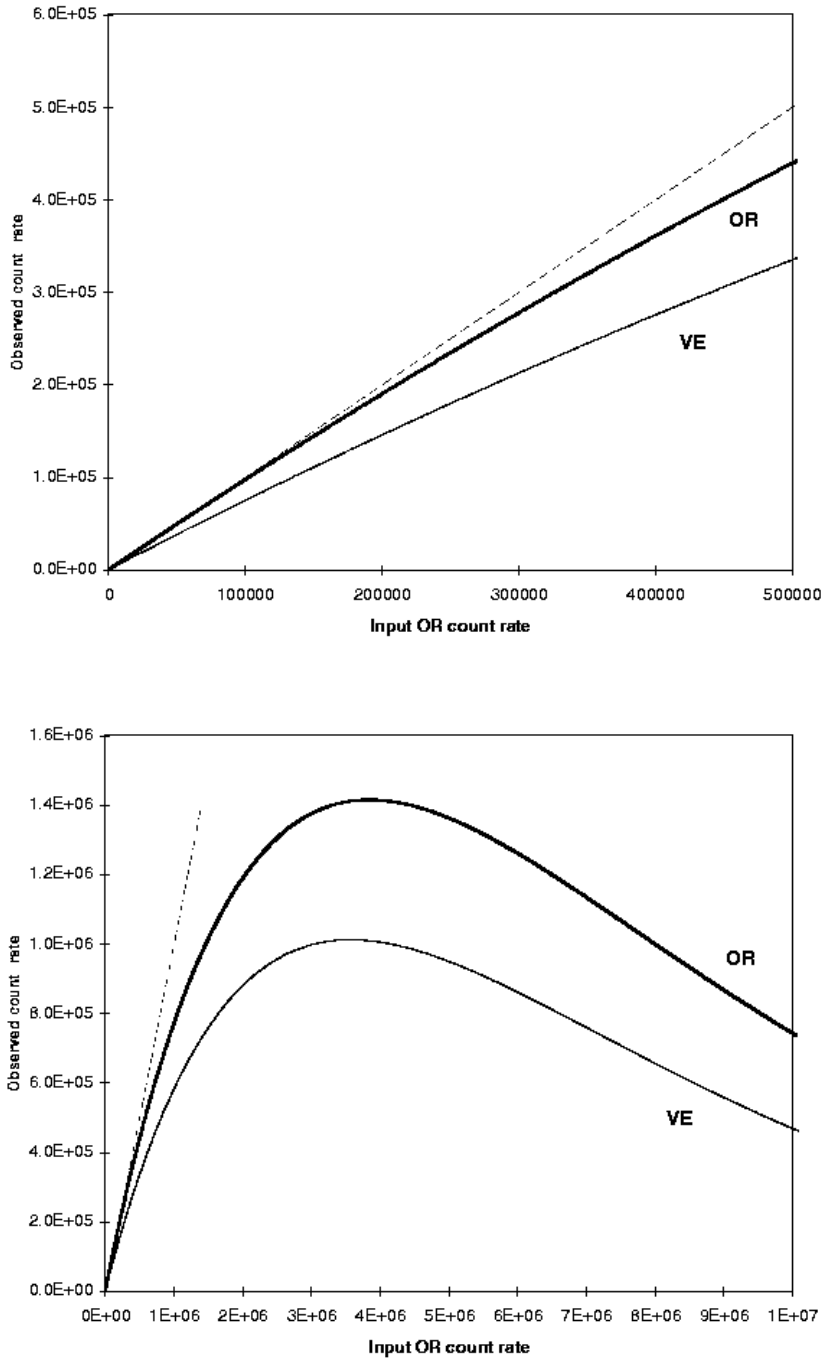

Hardware shutter

Detector Shutters

Of the three STIS detectors, only the CCD has an integrated shutter to protect the detector from illumination in the periods between exposures and during CCD readout, and this shutter is located in front of the detector. In order to protect the MAMA detectors from over-illumination, the current baseline is to use the Calibration Insert Mirror (CIM) mechanism, which blocks the external light path, as a shutter for the MAMAs.

Bright Earth Shutter

In response to concerns about UV illumination of the correction mirror which might lead to polymerization of contaminants on the mirror during the first months after the Servicing Mission, a new shutter assembly has recently been added to STIS. This shutter is located ahead of the first correction mirror and, when closed, will prevent external light reaching the spectrograph's optics. The shutter is not integrated with the STIS on-board control system but, instead is controlled via the RIU box. Initially, this shutter will be used only for the protection of STIS from bright earth illumination, however, it is expected that it will eventually be incorporated into the STIS bright object protection scheme.

NUV MAMA photocathode

The NUV MAMA was originally intended to be shuttered electronically by reversing the photocathode bias to prevent photoelectrons from reaching the MCPs (see Figure 2). This technique was expected to provide full protection for the NUV MAMA, effectively providing a shutter. Concerns regarding the cycling of high voltages on the MAMA, however have now precluded its use as a means of shuttering the NUV MAMA.

FUV MAMA Repeller

In the case of the FUV MAMA, reversing the repeller grid voltage will reduce incident photoelectrons at the MCP by about a factor of 40%. Some consideration has been given to using the repeller to attenuate the secondary photoelectron flux, but once again concerns regarding the cycling of high voltages on the MAMA, however have now precluded its use as a means of partially shuttering the NUV MAMA.

3. MAMA damage mechanisms

Permanent Damage

Depending upon the degree of over-illumination, the effect of a bright object on a MAMA detector can range from relatively benign to catastrophic. The primary mechanism for catastrophic damage to a MAMA detector is electrical breakdown within the MCP channels

and a reduction in vacuum pressure, due to the liberation of significant amounts of gas from the channel walls. This is expected to occur in cases where the detector is severely over-illuminated across a large fraction of its active area. The illumination level at which electrical breakdown might occur has not been determined experimentally with MAMA detectors, since they are limited resources. A conservative global damage limit of $1.5x10^6$ count/sec for a maximum of 1 second has been adopted by the STIS team. It is very possible that the detector may be able to sustain rates in excess of this rate. When gas is liberated from the channels walls, it may be subsequently reabsorbed by the MCP walls. Whenever a MAMA is over-illuminated, therefore, it is mandatory to wait at least 24 hours before bringing the detector back up to its nominal operating voltage. Longer waits may be advised at the discretion of the responsible instrument scientist, particularly following severe over-illumination of a detector.

Figure 5: MAMA images of a 30 μm spot obtained with increasingly higher input count rates.

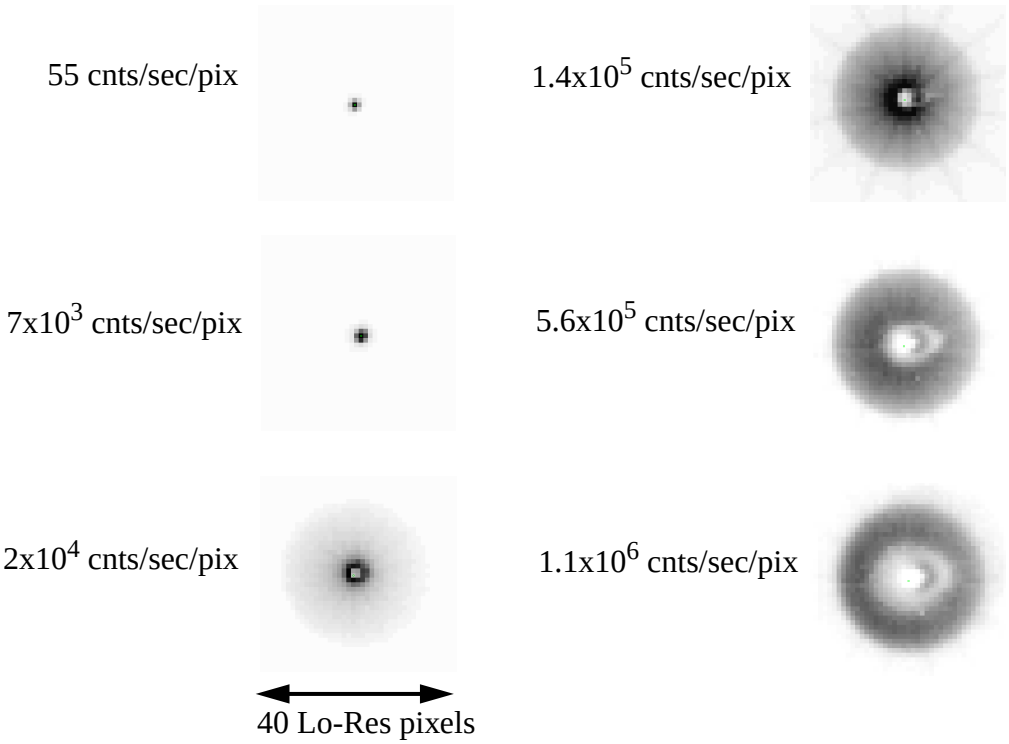

When a localized region (few pixels) of the MAMA detector is over-illuminated, the MCP channels are rapidly driven into saturation, liberating some gas in the affected channels. At higher local illumination levels a large halo appears around the saturated channels, due mainly to photoelectrons scattered at the MCP's inter-channel glass web. This process is illustrated in Table 5 which shows the result of illuminating an NUV MAMA with a point source of increasing input count rate. When the peak input count rate reaches ~10^4 counts/

sec/pix an extended halo, of ~50 pixels diameter, starts to appear around the core of the image. As the input count rate is increased, the count rate in the halo increases, while the core saturates and does not change, giving the image a characteristic ‘donut’ appearance.

In severe cases of local over-illumination, excessive count rates in the halo region (>50 counts/sec/pixel) can lead to the evolution of gas over a significant number of channels followed by electrical breakdown, and possibly permanent damage. In most cases of local over-illumination, the more immediate danger is that of accelerated aging of the MCP in the region illuminated. This causes a local sag in the MPC gain, resulting in an effective loss of QE and a depression in the flat field response.

MCP Lifetime Considerations

Rapid aging tests of MCPs has shown that they exhibit a long term loss of electron gain as increasing amounts of charge are extracted. The mechanism responsible for the loss of electron gain is believed to be a decrease in the secondary electron emission coefficient of the MCP glass, due to the removal of elements responsible for the conducting properties of the glass channels by electron scrubbing.

When a large drop in MCP gain occurs, the peak of the pulse height distribution (modal gain) shifts to lower gains. *Consequently, some real events are now discarded as they fall below the lower threshold (see Figure 6).* The lower threshold is applied to pulses in order to prevent low gain pulses from the exponential noise tail of the MCP’s pulse height distribution being processed as real events. For the MAMA detector, it is typically set at a level of $2x10^5$ electrons. The gain drop thus results in an effective loss of quantum efficiency, which can be easily corrected by increasing the MCP voltage to restore the desired modal gain. However, if the gain sag is isolated to a localized region of the MCP, it cannot be restored by increasing the MCP voltage and a permanent region of lower effective QE results.

Loss of MCP gain due to MCP aging is generally characterized as a function of the extracted charge in Coulomb/cm^2. The STIS team have defined a CEI specification of $8x10^{10}$ C/mm^2, which corresponds to $5x10^7$ counts/low resolution pixel at a rate of 50 counts/sec/pixel over the 5 year lifetime of STIS.

Optimum performance from MCPs is obtained by conditioning them prior to assembly of the detector. This is illustrated in Figure 7 which shows gain versus extracted charge relationships, obtained during conditioning of a C plate similar to those used by STIS detectors (Joseph et al. 1995). This figure illustrates how electron scrubbing is used to bring the initially steep gain vs. extracted charge relationship into a regime where it is more stable and suitable for extended use in a photon counting detector i.e. where relatively large amounts of extracted charge produce small changes in MCP gain.

Figure 6: A schematic diagram of a MAMA pulse height distribution (PHD). The PHD is gaussian with low (noise events) and high (ion events) energy components. The main gaussian distribution is isolated in the signal processing electronics by a lower threshold which rejects unwanted low gain events.The modal gain shifts its baseline to lower gain values as MCP aging occurs, and this results in true photon events being lost as they are shifted below the lower threshold.

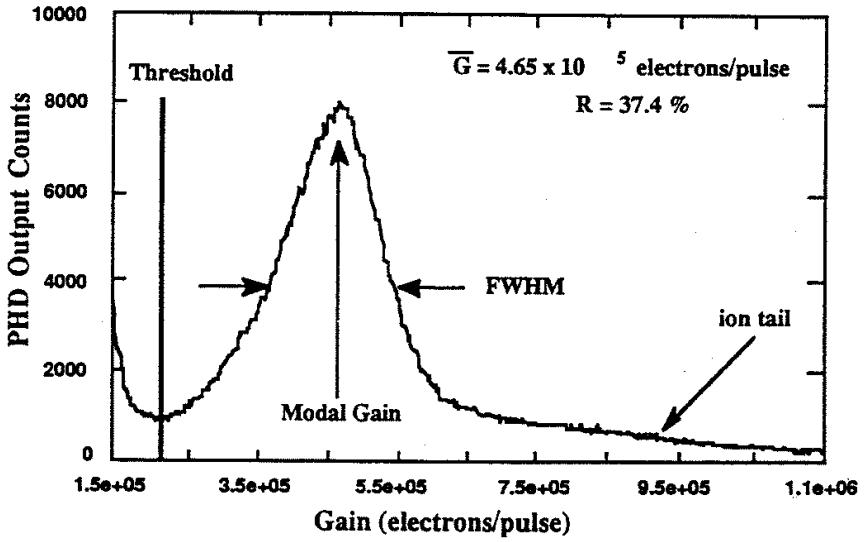

In Figure 7 the gain curve starts out very steep at an MCP voltage of 2150 V, but becomes more stable as charge is extracted and the MCP voltage is increased to compensate. The final resulting gain vs. extracted charge curve (top), at a MCP voltage of 2350 V, is relatively flat over the equivalent 5 year design lifetime of STIS.

As the STIS MCPs age, it will be possible to command the appropriate detector voltages to higher values. However, in order to ensure that long term loss of MCP gain in the STIS MAMAs can be compensated for by increasing the MCP voltage, it is important that the full active area of the detectors is aged at a uniform rate. This criterion is not met when the detector is either over-illuminated in a small region of the detector, or when bright spectral features are consistently imaged in the same region of the detector. The latter case will be prevented by applying offsets to the nominal MSM positions on a monthly basis so that spectra fall on a different area of the MAMA every month. The former requirement is more difficult to achieve and is the primary reason for operating a local rate monitor on the STIS MAMAs.

Recent local count rate testing of a NUV MAMA detector has produced a relationship which defines the exposure time to achieve a 1% loss of quantum efficiency at different input count rates (see Table 1). This table clearly demonstrates that local count rates below 50 counts/sec/pixel are unlikely to produce any local degradation of QE during STIS

observations of a few tens of orbits. However, input counts which are higher by less than an order of magnitude can produce local QE drops of >1% in what are likely to be typical exposure times for STIS. The FUV MAMA is expected to exhibit similar behavior.

Figure 7: The change in MCP gain as a function of extracted charge for a STIS C plate (provided by Check Joseph)

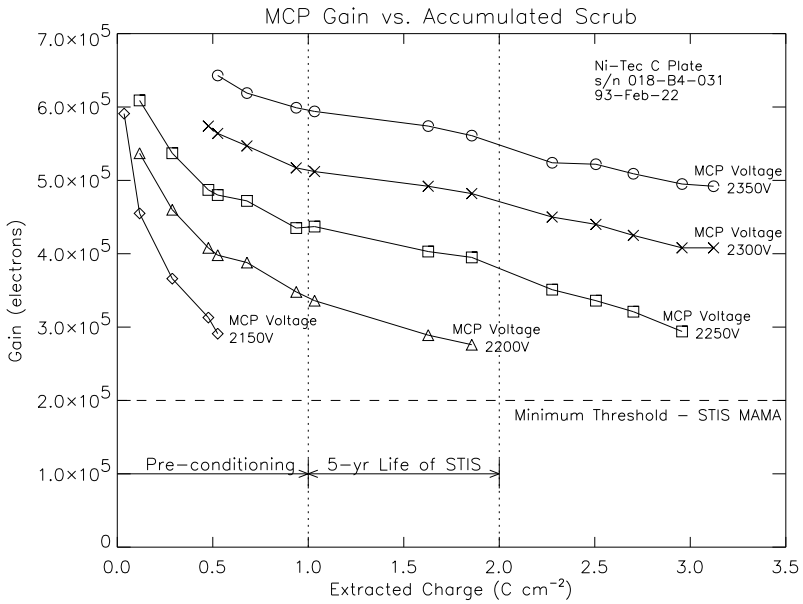

Table 1. Time to achieve a 1% QE loss for different input counts rates

Observing rate Counts/sec/pixel	Time to DQE loss (minutes)
50	36111
165	720
200	861
400	407
798	41
1189	10
2979	7
6306	6.6
15800	2.5
64500	2.4
238000	1.5

Ion feedback

In the case of the NUV MAMA detector, it is also possible for ions produced in the MCP to be accelerated into the photocathode, and damage it. This damage mechanism appears as a depression in the flat field response. The curvature of the MAMA MCPs is designed to preclude a clear path for ions liberated deep in the MCP, however, it is likely that some will still reach the photocathode when the MCP operates at very high input count rates. Ion feedback has the potential to damage the CsTe photocathode in conditions of both local and global over-illumination of the detector. It will manifest itself as loss of QE from the photocathode and appear in detector flat fields.

4. Hardware Protection of the MAMAs: Global Rate

STIS has two different methods of monitoring the global count rate and shutting down the detector if safe count rates are exceeded. These methods are the Bright Scene Detection (BSD) system and the Software Global Monitor (SGM). The requirements and capabilities for global count rate protection are summarized in Figure 8 (ISR-96-24).

Figure 8: Global trigger levels for MAMA Bright Object Protection

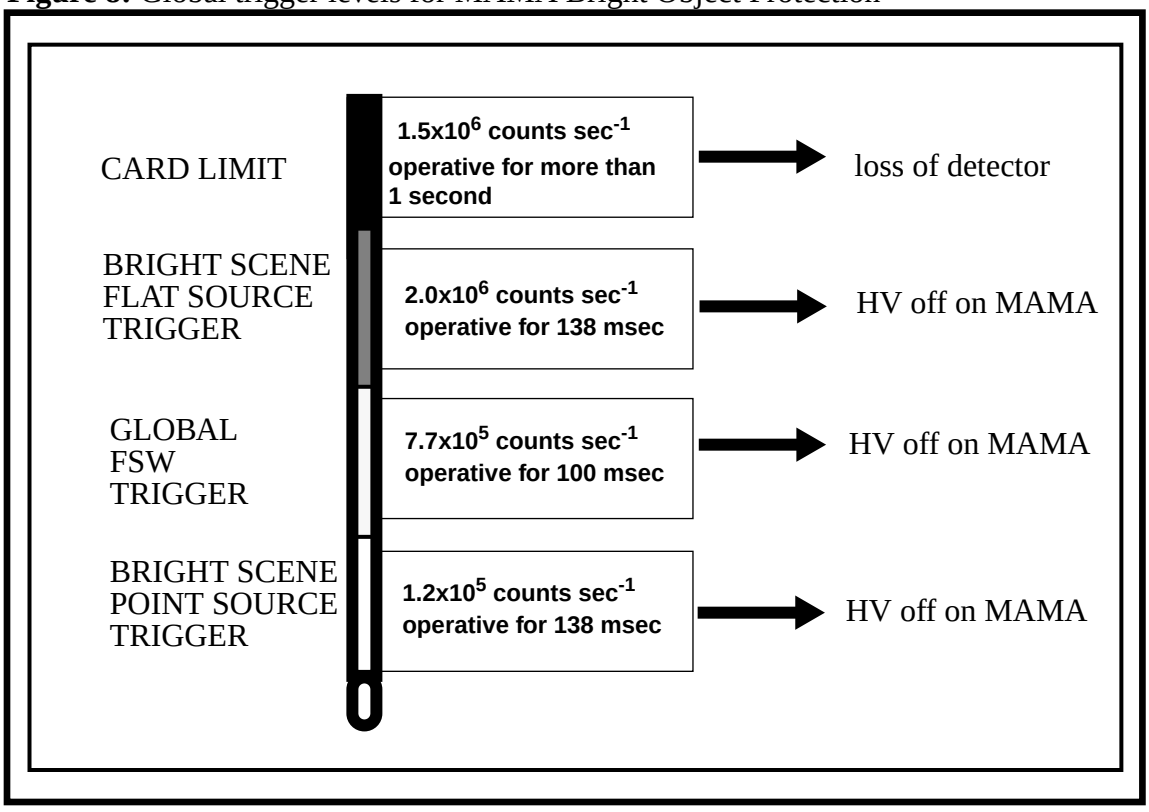

Bright Scene Detection (BSD)

The BSD is implemented in the MAMA electronics and can not be changed without a hardware modification to the system. The BSD was originally intended to provide the pri-

mary method of protection against over-illumination of the MAMAs, but concerns regarding its implementation led to the addition of the SGM. The BSD's primary value is that it provides some measure of protection when input count rates levels are high enough to saturate the decode chip and paralyze the SGM.

The BSD works by monitoring the output of two anode wires, designated W8 and W24, which run parallel to the MAMA axis1. The pixel locations of the two anode wires are summarized in Table 2. Coverage of the MAMA field of view is limited to two rows of pixels (Lo-Res) every 32 rows of pixels (Lo-Res), giving rather sparse coverage of the MAMA field of view. The two anode wire outputs are fed to charge amplifier/discriminator circuits. The discriminators are input to independent counters which each have a reset time of 138 ms. A count rate in excess of 16200 counts per 138 milli-second interval will set the counter output, which leads to the immediate shutdown of the detector high voltage. The counters from W8 and W24 are connected using an OR circuit, so either counter, or both will initiate a BSD event to the MCE. The BSD is always operational when the MAMA detectors are powered on. It can, however, be disabled via stored commands sent to flight software.

For the typical fold distribution of a nominal MAMA tube, any individual W amplifier will count at approximately 1/17th the total event rate on the detector, for a uniform input over the format (flat field illumination). Hence, the 117,400/second limit for each amplifier corresponds to a global limit of 17 x 117,400 = 2,000,000/second event rate for the flat field case.

For non-uniform illumination of the detector, the factor of 17 scaling does not apply. A narrow spectrum (1st Order) running in the same direction as the W anode lines can miss the monitored anodes completely. Alternatively, if the spectrum happens to lie on a row of pixels connected to one of the monitor amplifiers, hardware safing of the high voltage can occur at a count rate of 117,400 per second. As the monitor anode lines are only separated by 32 pixels, and the typical spatial extent of a 1st order spectrum is about 4 pixels wide, a first order spectrum with a count rate greater than 117,400 per second has a very significant probability of safing the detector if the dispersion direction is parallel with the W anodes. This is indeed the case, since the W anodes run in the MAMA Y axis, corresponding to the dispersion direction of the first-order spectroscopic modes of STIS. Hence, first order spectra with >117,400 counts/second in these modes have the potential to safe the MAMAs.

In summary, the BSD's role is to provide protection at count rate levels where the SGM becomes non-linear or saturates i.e. $>10^6$ counts/sec. It is, however, designed for uniform illumination of the detector's field of view and does not work well, for instance on point sources which are imaged on pixels in-between the monitored rows. The BSD also presents something of a problem in that its implementation means that 1st order spectra lying along a monitored row can trigger at count rates of ~120,000 counts/sec. Finally, the BSD

it is also relatively slow, with a sample time of 0.138 seconds.

Table 2. Row locations of the W8 and W24 anodes used by the BSD hardware

	W8	W24
1	15,16	47, 48
2	83,84	115, 116
3	151,152	183, 184
4	219, 220	251, 252
5	287, 288	319, 320
6	355, 356	387, 388
7	423, 424	455, 456
8	491, 492	523, 524
9	559, 560	591, 592
10	627, 628	659, 660
11	695, 696	727, 728
12	764, 765	795, 796
13	831, 832	863, 864
14	899, 900	931, 932
15	967, 968	999, 1000

Software Global Monitor

The SGM operates by monitoring the OR counter and shutting down high voltage to the detector if a specified OR count rate is exceeded. The OR counter is monitored because it counts all events detected by the MAMA which exceed the lower pulse size threshold. It has already been noted that the STIS signal processing electronics can process serial data rates up to $3x10^5$ counts/sec and is effectively the useful upper limit for scientific observations with STIS. Given the CARD restriction for global over-illumination of $1.5x10^6$ counts/sec for 1 second, the STIS science team have set the SGM trigger level, which shuts down the HV on the over-illuminated MAMA at $1x10^6$ OR counts/sec. This figure is an input OR count rate and, as is shown in Figure 4, corresponds to an observed OR count rate of 770,000 counts/sec due to non-linearity associated with the deadtime of the ASIC decoders (260 ns). The SGM trigger level is set at a value of 770,000 counts/sec. The valid event rate corresponding to an input OR count rate of 1,000,000 counts/sec is 580,000 counts/sec.

The SGM is commanded to be operational once the detector's high voltage has been

ramped to its nominal operational level. It is then continuously active until the detector high voltage is shut down again. It should be noted that some detector functional tests, such as those used in the MAMA anomalous recovery procedure and anode fold analysis selectively disable anode outputs so that the OR counter is no longer giving the true OR count rate. During these tests the SGM will not function correctly and the detector is potentially at risk.

The SGM is designed to provide the primary means of protection against illumination levels which could potentially lead to a failure of the detector i.e. global input count rates of $\geq 10^6$ counts/sec. It is faster than the BSD with a sample time of 0.1 seconds, but becomes rapidly ineffective at global count rates in excess of a $4x10^6$ counts/sec where it rolls over due to the 260 ns deadtime. As is shown in Figure 4, the observed OR count rate falls below the SGM trigger level of 770,000 counts/sec at an input OR count rate of $\sim 10^7$ counts/sec. It will provide the maximum benefit in catching sources which are brighter than the screening levels, by factors of ~4- 6.

5. Local rate monitor

The local rate monitor is designed to prevent observations being made with either MAMA which would exceed the current local rate limits summarized in Figure 9, and comprises two stages.

Figure 9: Local Flight Software Trigger and Screening Limits

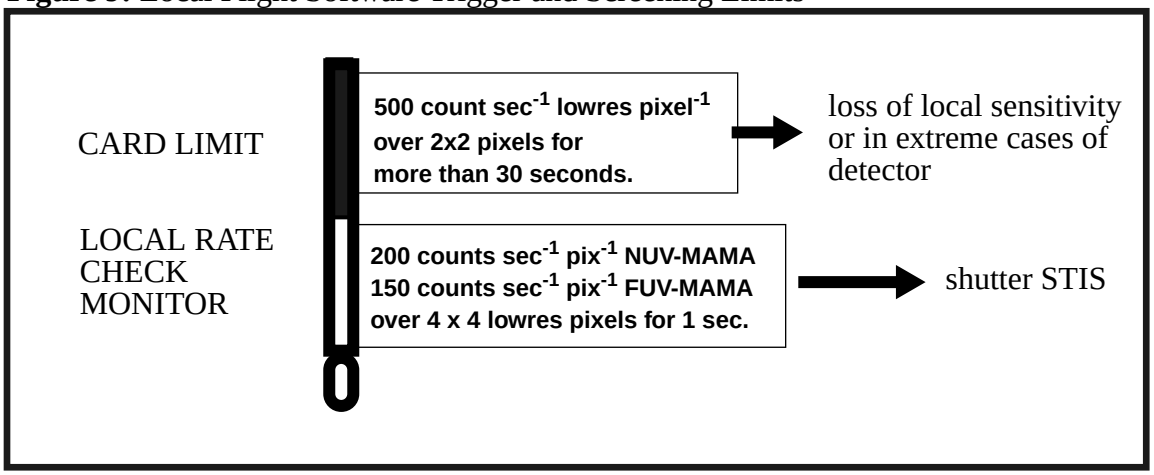

The local rate monitor has been implemented in FSW and operates via stored commanding. The two stage check is performed on a 300 ms image stored in MIE memory. The image is taken prior to every new observing configuration. In the first stage the MAMA image is rebinned, by 4x4 low resolution pixels, during readout to give an image of 256x256 superpixels. The superpixels are then examined to see if any violate a threshold value, summarized in Table 3. If the threshold value is violated, the exposure is aborted, the detector is shuttered, lamps are turned off and the status buffer is returned with the

appropriate error message. If none of the superpixels exceed the threshold value, the check proceeds to the second stage, in case the image happened to fall across superpixel boundaries. The second stage of the local rate check is dependent upon the instrumental configuration. On the basis of the optical element selected for the exposure the monitor categorizes the exposure as imaging, dispersion or cross-dispersion. For imaging observations a 2x2 superpixel checkbox is run across the image and any checkbox exceeding a threshold value (see Table 3) causes the detector to be shuttered so that the resulting exposure is a dark image. Calibration lamps are also turned off and the status buffer returned with the appropriate error message. In the case of a local rate violation the longest possible time for unshuttering, image acquisition, image analysis and MAMA shuttering is <9 seconds. The image header keyword `LRCFAIL` is also set to flag the image. Dispersion and Cross-Dispersion observations are the same, except that checkboxs of 1x2 and 2x1, respectively, are employed. The local rate procedure is shown schematically in Figure 10, to illustrate the flow of the image processing. If the local rate check is successful and the observation proceeds, the local rate image is dumped for future reference.

Currently, no allowance is made for the possibility of hot pixels or other image artifacts triggering the monitor. Such features have not been observed in the flight detectors STF1 and STE6 during ground testing. In the eventuality that such features did develop during the lifetime of the detector, a change to the flight software would be required. When a MAMA detector is unshuttered for the local rate monitor acquisition image, the other MAMA detector is no longer protected, and is not examined as part of the local rate monitor on the prime detector.

Local rate check threshold values

The threshold values for the local rate check monitor have been defined by the STIS IDT, on the basis of simulations made by Phil Plait and Don Lindler. The simulations were performed for (a) imaging modes, with a simulated point source, and (b) dispersed light modes, using various simulated spectra, including pure continuum, and emission line plus continuum in various ratios. Two image sizes were used in the simulations, 1.8 pixels FWHM and 2.2 pixels FWHM (Lo-Res pixels). The former is believed to best match the STIS UV modes, and was the value adopted in order to determine the onboard trigger limits. The resulting threshold values are summarized in Table 3.

These threshold values were adopted by the STIS Science Team on the basis that they provided the best performance over a range of conditions i.e. image types and location within a superpixel. Although the nominal trigger limits for the local rate monitor are 150 counts/sec/pixel and 200 counts/sec/pixel, there will be some spread in the actual level at which the local rate monitor triggers using these threshold limits. The FUV MAMA local rate check will trigger on peak count rates ranging from 136 counts/sec/pixel to 350 counts/sec/pixel, depending upon whether the exposure is an image or spectrum, while the NUV MAMA local rate check will trigger on values ranging from 136 counts/sec/pixel to 350 counts/sec/pixel, depending upon whether the exposure is an image or spectrum. Conse-

quently, there is not always a factor of four margin between the level at which STScI screens and the levels at which the local rate monitor triggers. While the local count rate monitor will trigger over a range of peak count rate values, the simulations indicate that the CARD will never be violated. The fact that in some cases, such as unresolved emission lines on a continuum, the local rate monitor might trigger at levels as high as ~350 counts/sec/pixel means that a 1% QE loss could be reached in ~11 orbits for such a source. The relatively high levels passed by the first stage of the FSW check (see Figure 3) should not produce any significant QE loss in the ~300 ms exposure taken for the local rate check image.

Table 3. Flight software values for local rate monitor thresholds.

			1st Pass	2nd Pass		
Band	Mode	Exposure time (milli-second)	Threshold#1 (cts/bin/ exposure)	Threshold#2 (cts/bin/ exposure)	Row Size	Column Size
FUV	image	300	180	180	2	2
FUV	dispersed	300	360	360	1	2
FUV	x-disp	300	360	360	2	1
NUV	image	300	225	225	2	2
NUV	dispersed	300	390	390	1	2
NUV	x-disp	300	390	390	2	1

6. References

Eberhardt, E. H. 1980, ITT Electro-Optical Products Division Technical Note No. 127.

Kasle, D. B., 1992, PHD thesis “An ASIC for high speed and high resolution decoding of multi-anode microchannel array detectors”, Stanford University.

Joseph, C., Argabright, V., Abraham, J., Dieball, D., Franka, S., Danks, A. and Woodgate, B., SPIE 2251, 248.

Wiza, J. L. 1979, Nuclear Instruments and Methods 162, 587.

7. Acknowledgments

We wish to thank the STScI STIS Commanding Group, Steve Kramer of GSFC, Vic Argabright and Charlie van Houten of Ball Aerospace and Tony Danks of Hughes STX for their advice and assistance in the preparation of this ISR.

Figure 10: Schematic showing Local Rate Monitor